J. Phys. Chem. A **2000,** *104,* 4030−4044

Exploration of the Mechanism of the Activation of $ClONO_2$ by HCl in Small Water Clusters Using Electronic Structure Methods

Jonathan P. McNamara, Gary Tresadern, and Ian H. Hillier*

Department of Chemistry, University of Manchester, Manchester, M13 9PL, United Kingdom

Received: September 13, 1999; In Final Form: January 5, 2000

High-level electronic structure calculations were used to study the mechanism of the reaction of $ClONO_2$ with HCl in neutral water clusters containing one to five solvating water molecules. For the reaction between molecular HCl and $ClONO_2$, the barrier decreases from 42 kcal mol^{-1} (uncatalyzed) to essentially zero when catalyzed by only two water molecules, where the reaction products involve Cl_2 and $HONO_2$. The calculations thus predict that the gas-phase reaction may be important in the stratospheric reactivation of $ClONO_2$. The reaction between $ClONO_2$ and solvated $H_3O^+Cl^-$, as on the polar stratospheric cloud (PSC) surface, was investigated with clusters involving up to seven water molecules. The ice-catalyzed reaction involves an ionic mechanism whereby charge transfer to $ClONO_2$ from the attacking nucleophile leads to significant ionization along the $Cl-ONO_2$ bond. The effect of the size of the first solvation shell of Cl^- is addressed by our calculations. In a cluster containing three waters and a five-water cluster structurally related to hexagonal ice, $ClONO_2$ reacts spontaneously with HCl to yield $Cl_2/HONO_2$ in the three-water reaction and Cl_2/H_3O^+-NO_3^- in the five-water-catalyzed reaction. The calculations thus predict that the reaction of $ClONO_2$ with HCl on PSC ice aerosols can proceed spontaneously via an ionic pathway.

1. Introduction

Polar stratospheric cloud (PSC) particles have been implicated as important sites for the heterogeneous catalysis of a number of atmospheric reactions[1,2] responsible for the depletion of ozone in the Antarctic stratosphere.[1−12] Of particular importance are those reactions involving the conversion of the reservoir species chlorine nitrate ($ClONO_2$) and HCl to photochemically labile Cl_2. Photolysis of Cl_2 leads to chlorine radicals capable of destroying ozone via efficient catalytic chain reactions. The PSC ice aerosols are classified as type I (nitric acid trihydrates, NAT) or type II (water ice). However, it is now widely accepted that the activation of both $ClONO_2$ and HCl can occur throughout the atmosphere on other atmospheric aerosols originating from volcanic eruptions, such as Mount Pinatubo (1991).[2]

The activation of $ClONO_2$ has been suggested to occur via a two-step mechanism (eqs 1a and 1b) or via a direct mechanism (eq 2).[6,13−22]

$$ClONO_2 + H_2O \rightarrow HOCl + HONO_2 \qquad (1a)$$

$$HOCl + HCl \rightarrow Cl_2 + H_2O \qquad (1b)$$

$$ClONO_2 {}^+ HCl \rightarrow Cl_2 + HONO_2 \qquad (2)$$

Both the hydrolysis reaction 1a, leading to hypochlorous acid (HOCl) and nitric acid ($HONO_2$), and reaction 2, which we refer to as the direct reaction, have been the subject of a number of experimental studies.[6,13−22]

The availability of modern laboratory apparatus allows the control of experimental parameters such as reactant partial pressure and substrate temperature so that conditions close to stratospheric ones can be simulated. Hanson,[18,22−24] Zhang,[25,26] and other workers[19−21,27−30] have used flow tubes to measure reaction probabilities or sticking coefficients (γ). The hydrolysis reaction and to a somewhat lesser extent, the direct reaction, have been extensively studied by the complementary techniques of Fourier transform (FTIR) or reflection−absorption infrared spectroscopy (RAIR) and mass spectrometric (MS) methods.[13−17] FTIR and RAIR spectroscopy allow direct observation and discrimination of different surface-adsorbed species, whereas MS methods allow determination of products evolved from surfaces. Methods to study the interaction of $ClONO_2$ with ion-containing water clusters[31−33] are also well documented.

Calculations indicating the polarized nature of the chlorine nitrate molecule[34] suggest that chlorine is the most accessible electrophilic site and is thus susceptible to nucleophilic attack by surface-adsorbed species,[6,13−22] with the reactivity of $ClONO_2$ being controlled by the relative nucleophilic/electrophilic strength of the species involved.

Under acidic conditions the direct reaction in eq 2 is believed to be dominant over hydrolysis (eq 1).[6,13−22] Wofsy et al.[35] propose an acid-catalyzed mechanism producing incipient Cl^+ or $NO_2{}^+$ leaving groups that then undergo ion−ion recombination with the solvated chloride anion of ionized HCl. The majority of experimental evidence suggests that at temperatures >50 K, ionized HCl is present at the surface[36−41] as well as in the bulk. Given the dynamic nature of the ice surface,[42] it is likely that adsorbates will be introduced into the bulk. Bianco and Hynes[43] propose two possibilities regarding the nature of the ionized HCl. Dissociation involving a proton transfer to an adjacent water molecule may lead to the formation of the $H_3O^+Cl^-$ contact ion pair; or alternatively, there is a high probability that the proton will be transferred far from the $ClONO_2$ reaction site such that the direct reaction

$$ClONO_2 + Cl^- \rightarrow Cl_2 + NO_3{}^- \qquad (3)$$

would then proceed. This reaction has been shown to be thermodynamically favorable in the gas phase.[44] Wincel et al.[30] have also shown reaction 3 to occur efficiently at temperatures

10.1021/jp9932261 CCC: $19.00

between 170 and 298 K, when the chloride ion is complexed with up to three water molecules.

At present there are no available experimental data regarding the rate of the direct reaction, yet Horn et al.[17] reported an instantaneous production of Cl_2 at 160 K, which indicates a facile reaction. However, the catalytic role of water in both homogeneous and heterogeneous catalysis has yet to be resolved and will be addressed in this work by focusing on the following issues:[6,13−22]

(i) Whether the direct reaction between $ClONO_2$ and HCl is ionic or molecular and particularly the role of water in this reaction.

(ii) The reasons for the low activation barrier inferred from the observed rapid reaction on PSC ice aerosols.

(iii) The role of the PSC ice aerosol in both catalyzing the reaction and whether the product nitric acid is ionic or molecular.

The structure and properties of $ClONO_2$ itself have been the subject of a number of theoretical investigations. The structure and harmonic frequencies of free $ClONO_2$ were calculated by Lee[45] and Ying and Zhao[46] using CCSD(T) and density functional (DFT) theories, respectively. The structure of the chlorine nitrate anion has been studied using Møller−Plesset perturbation theory (MP2) by Seeley et al.[47] Early ab initio investigations of the reactivity of $ClONO_2$ focused on the mechanism of hydrolysis. Lee et al.[48] studied the acid catalyzed mechanism proposed by Wofsy et al.[35] at the CCSD(T) level, whereas La Manna[34] calculated the structure of six isomers of $ClNO_3$ using Hartree−Fock (HF) and MP2 methods and proposed that the strongest interaction with water occurs along the Cl−O intermolecular axis. More recently, Bianco and Hynes[49] and Xu and Zhao[50,51] modeled the hydrolysis of $ClONO_2$ in small water clusters leading to solvated molecular HOCl and $HONO_2$ at the MP2//HF level. The latter authors highlighted the role of the ice surface in both structure catalysis and hydration of heterogeneous reactions, where the hydrolysis is compatible with the proposed ion-catalyzed mechanism.[6,13−22] However, Bianco and Hynes[49] have also identified the ionic products (HOCl and $H_3O^+NO_3^-$) along an MP2//HF/6-31+G-(d,p), STO-3G microsolvated reaction path, where the barrier is 3 kcal mol^{-1}. In accord with this result, the hydrolysis reaction leading to the ionic products has also been shown by DFT calculations to occur essentially spontaneously in a cluster containing six water molecules that is related to hexagonal ice.[52,53]

The direct reactivation of $ClONO_2$ has been of some interest theoretically. Haas et al.[44] found no barrier for the gas-phase reaction with the chloride anion (eq 3), whereas Mebel et al.[54] found that the barrier for the gas-phase reaction with molecular HCl (∼45−60 kcal mol^{-1}) became negative when catalyzed by NO_3^-. Bianco and Hynes[43] reported the results of ab initio calculations for the direct reaction on a model ice lattice containing nine water molecules. In agreement with experiment,[6,13−22] they calculated a barrier of 6.4 kcal mol^{-1} for the reaction of $ClONO_2$ coordinated to the ion pair ($H_3O^+Cl^-$), leading to the ionic products $H_3O^+NO_3^-$ and Cl_2. Moreover, in an ab initio study, Xu and Zhao[55] calculated the direct reaction to occur with essentially zero barrier in a relatively small water cluster. Other important atmospheric reactions have also been studied by ab initio methods.[56−72]

In this paper we present the results of ab initio (MP2) and DFT calculations to understand both the homogeneous gas-phase reaction and the heterogeneous PSC aerosol-catalyzed reaction of $ClONO_2$ + HCl. A number of important issues are addressed by our cluster models. The calculations indicate that the gas-phase reaction involving small water droplets where HCl is un-ionized occurs readily at stratospheric temperatures. For the reaction in larger clusters related to the ice surface, where HCl is ionized to form either the $H_3O^+Cl^-$ contact ion pair or the solvent-separated ion pair, a facile reaction is also predicted. The calculations indicate that the structure of the local adsorption site is important in effecting ionization of species involved in the reaction. Furthermore, our cluster models confirm the experimental observations that at stratospherically relevant temperatures, the final reaction products contain the ionized form of nitric acid $H_3O^+NO_3^-$.[6,13−22] Finally, in light of our calculations, the implications for stratospheric chemistry are discussed.

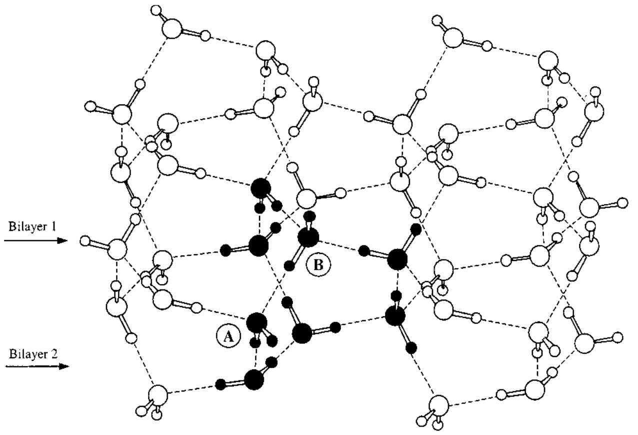

Figure 1. Fragment of proton-ordered hexagonal ice, showing water molecules (A, B) removed to accommodate chlorine nitrate.

2. Modeling Small Water Droplets and the Ice Surface

The construction and orientation of water molecules at the ice surface are largely unknown. When liquid water freezes at atmospheric pressure, the oxygen atoms comprise a wurzite lattice,[73] where the hydrogen atoms are distributed throughout the lattice along the O−O bonds according to the Bernal and Fowler ice rules.[74] The disorder in the proton positions exists down to 0 K and is responsible for the residual entropy at this temperature.[75]

The nature of the ice surface with particular reference to its role in low-temperature heterogeneous catalysis has been highlighted by a number of experimental studies. The structure of the external surface of an ice film, crystallized on a Pt(111) surface at 90 K, was investigated by Materer et al.[76] Using a variety of techniques [low-energy electron diffraction (LEED), molecular dynamics (MD), and ab initio calculations], they found that the ice surface had full bilayer termination (Figure 1). Devlin and Buch used FTIR spectroscopy and MD/Monte Carlo simulations to investigate small adsorbate interactions with ice-like surfaces.[77−81] They assigned surface molecules to one of three categories; three coordinated molecules with either dangling hydrogen or dangling oxygen coordination and four coordinated molecules with distorted tetrahedral geometry. Buch et al.[81] also noted that both simulation and experiment indicate that the surface of ice contains rings of water molecules large enough to accommodate several adsorbate species.

The bulk properties of the condensed phase have been the focus of a number of theoretical studies.[73,75,82−85] In particular, MD simulations have been successful in elucidating the ionization of HCl at the ice surface.[36] However the interaction of small atmospherically relevant species, such as HOCl and HCl, with the ideal ice surface have also been studied by electronic structure methods.[58,60] Geiger et al.[58] used a four-water cluster

TABLE 1: Geometric Parameters of $ClONO_2$

	geometric parameter[a]						
method/basis set	$r(Cl_1-O_2)$	$r(O_2-N_3)$	$r(N_3-O_4)$	$r(N_3-O_5)$	$\angle(Cl_1O_2N_3)$	$\angle(O_2N_3O_4)$	$\angle(O_2N_3O_5)$
HF							
6-311++G(d,p)	1.663	1.372	1.165	1.166	116.4	111.0	118.4
6-311++G(3df,3pd)	1.642	1.368	1.164	1.163	116.0	111.1	118.3
MP2							
6-311++G(d,p)	1.700	1.557	1.192	1.190	112.0	107.8	116.9
6-311++G(3df,3pd)	1.668	1.547	1.188	1.185	111.2	108.0	116.3
B3LYP							
6-311++G(d,p)	1.711	1.516	1.189	1.188	113.9	108.5	117.6
6-311++G(3df,3pd)	1.679	1.513	1.186	1.184	113.4	108.8	117.2
other							
CCSD(T)/TZ2P[b]	1.707	1.511	1.195	1.197	111.9	108.7	117.8
experiment[c]	1.673	1.499	1.196	1.196	113.0	108.8	118.6

[a] Bond lengths (Å), angles (deg). Refer to Figure 2 for atom labeling. All levels of theory calculate $ClONO_2$ to be planar. [b] Lee[45]. [c] Vibrationally averaged gas-phase $ClONO_2$ structure.[45]

excised from the ideal surface of hexagonal ice. Similarly Brown and Doren[60] studied the interaction of HOCl with both $(H_2O)_4$ and $(H_2O)_{26}$ cluster models excised from the hexagonal ice surface. The latter models were constrained to retain the structural features of the ideal surface. In view of the proposed dynamic nature of the ice surface,[42] the mechanisms of atmospheric reactions were also explored in small water clusters by high-level ab initio techniques. Vincent et al.[64] elucidated the mechanism of oxidation of SO_2 by H_2O_2 in water droplets, whereas Smith et al.[65] examined the process of acid dissociation in water clusters. Our recent calculations concerning the hydrolysis of $ClONO_2$,[52,53] in addition to the work of Bianco and Hynes,[49] have shown these prototypical clusters to suitably reproduce the observed reactivity of the PSC surface and small water droplets. Models that represent the local adsorption site by fragments excised from an ideal ice lattice[58,60] may not account for the solvating effect of the ice surface beyond the adsorption site. As the foreign molecule approaches the ice surface, there is a high probability that it will be at least partially solvated by either surface-bound H_2O[42] or solvated within a ring of water molecules.[81] In view of Buch's findings[81] and the dynamic nature of the ice surface,[42] we chose to study the direct reaction in water clusters, which are relevant to the study of reactions in small water droplets and on the PSC aerosol surface.

3. Computational Methods

The calculations presented herein were carried out using the Gaussian 94[86] and Gaussian 98[87] suites of programs. Electron correlation was included at the DFT (B3LYP)[88−90] and MP2[91] levels. For the larger systems studied, DFT was chosen to minimize computational expense, MP2 optimization being too time-consuming for systems with ~300 basis functions. The B3LYP functional was chosen because previous calculations by Ying and Zhao[46] and our recent studies[52,53] in which the calculated structure of free $ClONO_2$ at this level was shown to be of comparable quality to that of the CCSD/TZ2P method[45] (Table 1). All DFT optimizations used the flexible 6-311++G-(d,p) gaussian basis set, because of recent electronic structure calculations that show that both polarization and diffuse functions are required to describe hydrogen bonded systems; with smaller basis sets often leading to preferential stabilization of ionic species.[64] For the larger systems, single-point energy calculations were carried out at the MP2/6-311++G(3df,3pd)//B3LYP/6-311++G(d,p) level for comparison. Thus, the calculations described are at a significantly higher level than those previously reported.[43] Stationary structures were characterized as minima or transition structures on the potential energy surface by calculation of harmonic vibrational frequencies. Intrinsic reaction coordinate calculations were performed to confirm that the transition structures connected the reactant and product minima. Free energies were calculated within the perfect gas, rigid rotor, harmonic oscillator approximation.

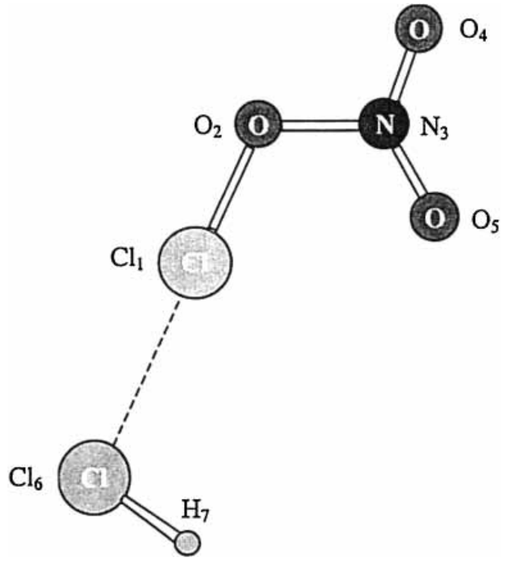

Figure 2. Core reaction system.

4. Computational Results

In discussing the various structures we refer to the atom-labeling scheme of the reactant pair (Figure 2), which contains $ClONO_2$ and the attacking nucleophile HCl. All of the structures are denoted by the number of complete water molecules they contain before reaction. Individual structural parameters are at the B3LYP/6-311++G(d,p) level unless otherwise stated. Relative energies and reaction barriers given in the proceeding text are free energies at 180 K, a temperature appropriate to the experimental conditions.[6,13−22] The reaction energy is defined as the difference in energy between the reactant and product structures.

A. Gas-Phase $ClONO_2$. First we consider the structure of free $ClONO_2$. Table 1 contains the optimized structure of $ClONO_2$ calculated using the HF, MP2, and DFT (B3LYP) methods. Both the experimental structure[45] and that from a coupled cluster calculation by Lee[45] are given for comparison. The structure of $ClONO_2$ at the HF/6-311++G(d,p) level shows

TABLE 2: Mulliken Charges (e) B3LYP/6-311++G(d,p) of Reactant Pair (Figure 2)

	atomic charge[a]							total fragment charge				
reaction/structure	Cl_1	O_2	N_3	O_4	O_5	Cl_6	H[b]	$ClONO_2$	HCl	Cl_2	H_2O[c]	$HONO_2$
$ClONO_2$	0.08	0.07	−0.26	0.03	0.08			0.00				
$ClONO_2 + HCl$[d]												
reactants	0.09	0.09	−0.28	0.04	0.07	−0.16	0.15 (7)	0.01	−0.01			
transition state	0.08	0.14	−0.41	0.08	0.14	−0.25	0.22 (7)	0.03				
products	0.05	0.00	−0.32	0.01	0.06	−0.01	0.21 (7)			0.04		−0.04
$ClONO_2 + HCl\cdot(H_2O)$[e]												
reactants	0.08	0.11	−0.30	0.04	0.02	−0.19	0.20 (7)	−0.05	0.01		0.04	
transition state	0.01	0.12	−0.34	0.02	−0.10	−0.25	0.17 (7)	−0.29			0.37	
products	−0.02	−0.02	−0.30	−0.01	−0.08	0.03	0.43 (9)			0.01		0.02
$ClONO_2 + HCl\cdot(H_2O)_2$ (isomer 1)[f]												
reactants	0.09	0.11	−0.33	0.03	0.00	−0.25	0.24 (7)	−0.10	−0.01		0.09	
transition state	0.07	0.12	−0.35	0.02	−0.04	−0.31	0.25 (7)	−0.18			0.23	
Products	−0.06	−0.07	−0.35	0.01	−0.03	0.02	0.46 (12)			−0.04		0.02
$ClONO_2 + HCl\cdot(H_2O)_2$ (isomer 2)[g]												
reactants	0.08	0.10	−0.31	0.03	0.03	−0.24	0.21(7)	−0.07	−0.03		0.08	
transition state	0.05	0.12	−0.33	0.02	−0.03	−0.33	0.22 (7)	−0.17			0.26	
products	−0.04	−0.03	−0.31	0.01	−0.09	0.03	0.46 (9)			−0.01		0.04

[a] Refer to figures for atom labeling. [b] (In parentheses) atom label. [c] Atoms O_8, H_9 and H_{10}. [d] Figure 4. [e] Figure 5. [f] Figure 6. [g] Figure 7.

important inadequacies, particularly with respect to the O_2-N_3 bond length. This length differs by ~0.13 Å from the experimental value and thereby overestimates its ionicity; however, at this level, the Cl_1-O_2 bond distance (1.66 Å) is quite close to the experimental value (1.67 Å). The addition of further polarization functions [HF/6-311++G(3df,3pd)] decreases both the Cl_1-O_2 and O_2-N_3 distances, thus increasing the discrepancy between calculation and experiment. In contrast, the MP2/6-311++G(d,p) geometry has Cl_1-O_2 and O2−N3 bond lengths of 1.70 and 1.56 Å, respectively, which are somewhat longer than the corresponding experimental values of 1.67 and 1.50 Å, respectively. In the B3LYP/6-311++G(d,p) structure, the O_2-N_3 bond length (1.52 Å) is very close to the experimental value (1.50 Å) and is in accord with the MP2 result, with the Cl_1-O_2 bond of length 1.71 Å being overestimated. Expansion of the basis [B3LYP/6-311++G(3df,3pd)] results in a structure that is in excellent agreement with experiment, with Cl_1-O_2 and O_2-N_3 bond lengths of 1.68 and 1.51 Å, respectively. The Mulliken charges [B3LYP/6-311++G(d,p)] for $ClONO_2$ (Table 2) indicate a polarization of charge, with a large negative charge of −0.26 on the nitrogen and a small positive charge of 0.08 on the chlorine. Having considered the structure of free $ClONO_2$, we now briefly consider the reactivity of HCl solvated in small water clusters relevant to the study of the reaction of $ClONO_2$ and HCl in such clusters.

B. $HCl\cdot(H_2O)_3$ and $HCl\cdot(H_2O)_4$. Recent ab initio and Monte Carlo investigations have revealed that in smaller water clusters with up to three solvating waters, un-ionized HCl is favored,[59] whereas in clusters containing at least four water molecules, ionized HCl is favored.[65−67] Solvation of HCl in a three-water ring (Figure 3a) leads to partial ionization of HCl (H−Cl 1.36 Å, isolated molecule 1.29 Å) and the addition of a further ring water (isomer 1, Figure 3b) enhances this effect, which is in agreement with previous investigations.[59] We identified two other minimum energy structures containing HCl solvated by four water molecules. Isomer 2 (Figure 3c) is essentially the $HCl\cdot(H_2O)_3$ cluster with an extra solvating water (A) and contains un-ionized HCl. In contrast, isomer 3 (Figure 3d), which is also based on the $HCl\cdot(H_2O)_3$ cluster, contains the ion pair $H_3O^+Cl^-$, with the molecular form of the acid (HCl) being unstable in this cluster. Evidently, for isomer 3, the extra bridging water (A) is able to stabilize both H_3O^+ and Cl^-, each of these species being stabilized by three hydrogen bonds. We also note the cooperative nature of the ionization process where in parallel with the lengthening H−Cl bond upon solvation, there is a notable shortening of the ring hydrogen bonds. At 180 K, isomers 2 (Figure 3c) and 3 (Figure 3d) containing the ionized and un-ionized forms of HCl, respectively, are essentially isoenergetic, whereas the single-ring structure (Figure 3b) is ~2−3 kcal mol^{-1} lower in energy. Thus, in agreement with previous studies,[59,65−67] we have shown that HCl can exist in both ionized and un-ionized forms depending not only on the number of solvating waters but on their structural arrangement. We now consider the reaction of $ClONO_2$ and HCl in the absence of water.

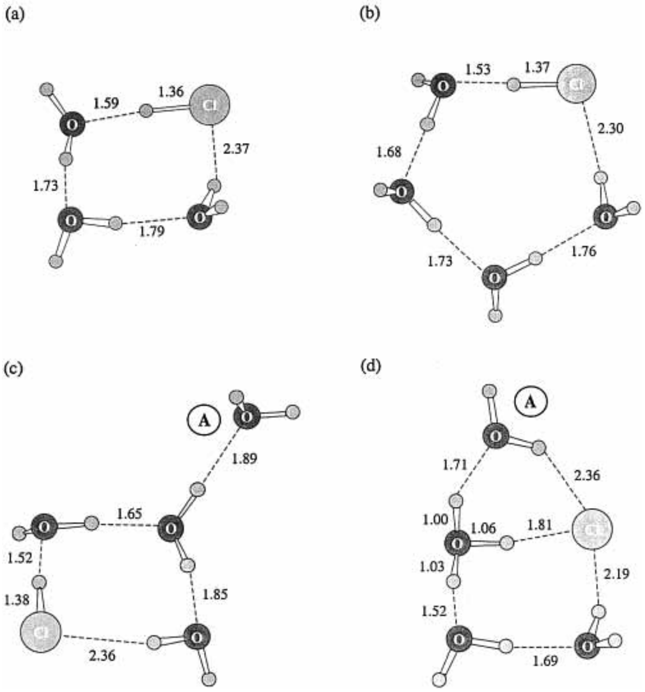

Figure 3. HCl solvated by (a) three water molecules and four water molecules, (b) isomer 1, (c) isomer 2, and (d) isomer 3. In this and subsequent figures, distances are in angstroms (Å) and correspond to the optimized B3LYP/6-311++G(d,p) geometries unless otherwise stated.

C. $ClONO_2 + HCl$. A number of recent works[49−51,55] have modeled the reactions of $ClONO_2$ using relatively low levels

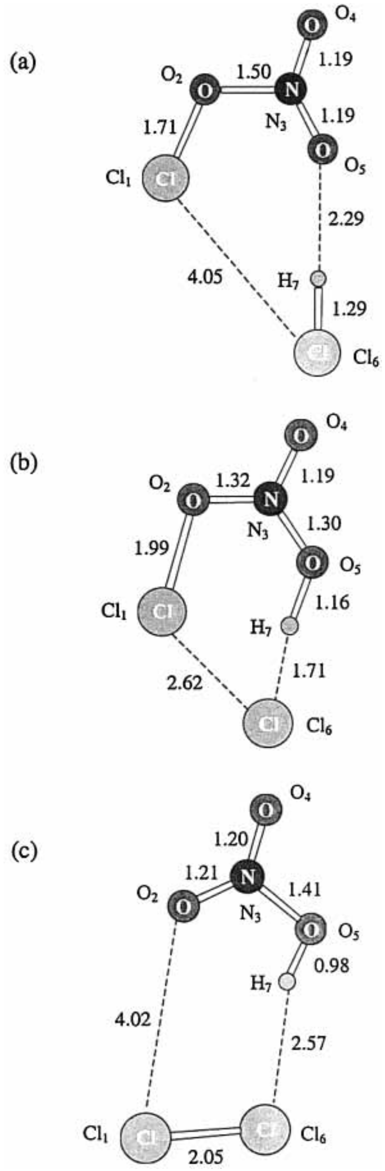

Figure 4. Stationary structures for reaction of $ClONO_2$ with HCl: (a) reactants, (b) transition state, and (c) products ($Cl_2/HONO_2$).

of calculation [e.g., HF/6-31G(d)]. Thus, we calculated structures at the HF level for comparison and to extend our study to clusters involving explicit water molecules that may involve the formation of ion pairs; a large basis including diffuse functions was employed [6-311++G(d,p)] to correctly describe anionic species.[65] Furthermore, calculations on free $ClONO_2$ (Table 1) indicate that to correctly describe the Cl_1-O_2 bond, both f and d polarization functions must be included [6-311++G-(3df,3pd)]. Therefore, we calculated stationary structures with both these large basis sets to quantify the energetic and structural effects of additional polarization and diffuse functions. The stationary structures calculated at the B3LYP/6-311++G(d,p) level are shown in Figure 4 and are representative of the corresponding structures calculated at other levels. We now discuss the structures and barriers obtained at the B3LYP/6-311++G(d,p) level and compare them with the corresponding barriers and structures calculated at the HF and MP2 levels with this basis (Tables 3 and 4).

Our study of the direct reaction in the gas phase follows that reported by Mebel and Morokuma[54] (also Xu and Zhao[55]) who found barriers of ~45 kcal mol^{-1} (B3LYP/6-31+G(d)) and ~64 kcal mol^{-1} [MP2/6-31+G(d)] for the pathway we have studied. Our calculations show the effect of different levels of theory with barriers of 65.7 (HF), 55.9 (MP2), and 41.8 kcal mol^{-1} (B3LYP). There is also a variation in the calculated reaction energies; HF predicts the product structure ($Cl_2/HONO_2$) to be lower in energy than reactants (24.8 kcal mol^{-1}), whereas MP2 calculates a much smaller value (9.8 kcal mol^{-1}), and the reaction energy is -13.8 kcal mol^{-1} at the DFT level. Notably, the size of the basis used with a particular method results in only small changes in the calculated barriers and reaction energies. The inclusion of thermodynamic corrections (180 K) yields barriers and reaction-free energies that do not radically differ from the corresponding internal energy values (0 K; Table 3). We find that the reaction follows essentially the same pathway at all levels of calculation; that is, in the reactant complex, HCl is hydrogen bonded to O_5 of $ClONO_2$, and the reaction occurs via a high-energy transition state containing species akin to Cl^- and protonated $ClONO_2$. This transition state leads to the weakly bound molecular $Cl_2/HONO_2$ product complex. The structure of $ClONO_2$ in the reactant complex (Figure 4a) is closely related to that of the free molecule (Table 1), with the charge distribution in the complexed $ClONO_2$ being essentially the same as that in the isolated molecule (Table 2) and with HCl being somewhat polarized with small charges of -0.16 and 0.15 on Cl_6 and H_7, respectively. The transition structure (Figure 4b) is characterized by an extension of the Cl_1-O_2 bond and a transfer of H_7 from Cl_6 to O_5 of $ClONO_2$. The structural parameters of the transition structure are close to those at the MP2 level; namely, the increased Cl_1-O_2 distance of 1.99 Å (1.71 Å reactant complex) and the compressed O_2-N_3 bond (from 1.50 to 1.32 Å) of the forming $HONO_2$. However, the length of the forming Cl_2 bond (2.62 Å) is somewhat different to the MP2 value of 2.46 Å. Thus, Cl_2 formation is more advanced in the MP2 transition structure. The breaking Cl_6-H_7 bond (1.71 Å) is notably longer than the forming O_5-H_7 bond (1.16 Å), which is consistent with the ionization of HCl to form Cl^- and protonated $ClONO_2$. Evidence supporting charge separation in the transition structure is afforded by a Cl_6 charge of -0.25 and a net charge of 0.25 on the protonated $ClONO_2$ entity (Table 2). The product complex (Figure 4c) involves weakly bound Cl_2 and molecular nitric acid ($HONO_2$) as evidenced by the nonbonded Cl_1-O_2 and Cl_6-H_7 distances of 4.02 and 2.57 Å, respectively. For the MP2 surface, the Cl_1-O_2 nonbonded distance is somewhat shorter (3.45 Å), indicating a stronger interaction.

Finally, at all levels used (HF, MP2, DFT), the extension of the basis to include more polarization functions to better describe $ClONO_2$ [6-311++G(3df,3pd)] results in small changes in the structures. For example, in the transition structure (DFT), the Cl_1-O_2 and Cl_1-Cl_6 distances both decrease to 1.93 and 2.57 Å, respectively, compared with 1.99 and 2.62 Å, respectively, with the smaller basis [6-311++G(d,p)]. Having considered the effect of model of electron correlation and basis sets on the energetics and structures of the prototype reaction in the absence of water, we now consider the catalytic effect of solvation by a single water molecule.

D. $ClONO_2$ + $HCl\cdot(H_2O)$. In view of the high-energy barrier calculated for the reaction of $ClONO_2$ with HCl (Table 3), we studied the catalytic effect of the addition of a single water molecule to our model reaction system (Figure 4a) to yield a structure (Figure 5a) similar to that found previously in our study of the hydrolysis of $ClONO_2$.[52] As for the uncatalyzed reaction, we examined the effect of different models of electron correlation and different basis sets on both the structures and energetics

TABLE 3: Reaction Energies and Barriers (kcal mol^{-1}) and Transition State Imaginary Frequencies (i cm^{-1})

method/basis set	imaginary frequency	internal energy (0 K)		free energy (180 K)	
		barrier	reaction energy	barrier	reaction energy
$ClONO_2 + HCl$					
HF					
6-311++G(d,p)	376	64.0	−24.8	65.7	−24.8
6-311++G(3df,3pd)	326	62.0	−25.7	64.0	−25.1
MP2					
6-311++G(d,p)	1674	54.8	−12.5	55.9	−9.8
B3LYP					
6-311++G(d,p)[a]	1159	40.9	−16.1	41.8	−13.8
6-311++G(3df,3pd)	1123	41.7	−17.7	43.0	−14.2
$ClONO_2 + HCl{\cdot}(H_2O)$					
HF/6-311++G(d,p)	298	25.3	−28.3	34.7	−22.7
MP2/6-31++G(d,p)	188	16.7	−13.4	21.0	−11.0
B3LYP/6-311++G(d,p)[b]	179	6.1	−18.1	5.1	−20.6
$ClONO_2 + HCl{\cdot}(H_2O)_2$ (isomer 1)[c]					
B3LYP/6-311++G(d,p)	194	0.5	−18.8	1.1	−17.5
MP2/6-311++G(3df,3pd)[f]		3.3	−20.0	3.9[g]	−18.7[g]
$ClONO_2 + HCl{\cdot}(H_2O)_2$ (isomer 2)[d]					
B3LYP/6-311++G(d,p)	245	1.1	−18.8	2.1	−16.7
MP2/6-311++G(3df,3pd)[f]		3.7	−18.6	4.8[g]	−16.5[g]
$ClONO_2 + HCl{\cdot}(H_2O)_3$ (cluster 4)[e]					
B3LYP/6-311++G(d,p)	52	0.4	−7.7	−0.1	−17.4
MP2/6-311++G(3df,3pd)[f]		0.0	−14.8	−0.3[g]	−24.4[g]

[a] Figure 4. [b] Figure 5. [c] Figure 6. [d] Figure 7. [e] Figure 10. [f] Single-point energy evaluations using B3LYP/6-311++G(d,p) structures. [g] Includes thermodynamic correction at B3LYP/6-311++G(d,p) level.

TABLE 4: Geometric Parameters for $ClONO_2 + HCl$ Reaction

method/basis set	geometric parameter[a]						
	Cl_1-O_2	O_2-N_3	N_3-O_4	N_3-O_5	O_5-H_7	Cl_6-H_7[b]	Cl_1-Cl_6
HF							
reactants							
6-311++G(d,p)	1.664	1.367	1.162	1.171	2.377	1.271	4.261
6-311++G(3df,3pd)	1.643	1.364	1.161	1.167	2.468	1.266	4.212
transition state							
6-311++G(d,p)	1.794	1.288	1.138	1.283	0.998	2.205	2.671
6-311++G(3df,3pd)	1.753	1.289	1.137	1.276	0.999	2.209	2.641
products							
6-311++G(d,p)	3.515	1.184	1.165	1.332	0.950	4.030 (2.823)	2.001
6-311++G(3df,3pd)	3.409	1.182	1.163	1.327	0.949	3.923 (2.694)	1.975
MP2							
reactants							
6-311++G(d,p)[c]	1.702	1.542	1.191	1.193	2.280	1.275	4.006
transition state							
6-311++G(d,p)	1.991	1.321	1.208	1.292	1.197	1.618	2.457
products							
6-311++G(d,p)[c]	3.453	1.215	1.204	1.406	0.973	2.462	2.024
B3LYP							
reactants							
6-311++G(d,p)[d]	1.712	1.503	1.187	1.193	2.287	1.289	4.054
6-311++G(3df,3pd)	1.680	1.503	1.184	1.188	2.351	1.283	4.016
transition state							
6-311++G(d,p)[e]	1.992	1.322	1.189	1.300	1.158	1.708	2.622
6-311++G(3df,3pd)	1.928	1.325	1.185	1.295	1.154	1.727	2.567
products							
6-311++G(d,p)[f]	4.020	1.211	1.195	1.412	0.975	2.567	2.053
6-311++G(3df,3pd)	3.844	1.208	1.193	1.403	0.975	2.498	2.011

[a] Distances (Å). All structures essentially planar. Refer to Figure 4 for atom labeling. [b] (In parentheses) Cl_1-H_7. [c] Nonplanar. [d] Figure 4a. [e] Figure 4b. [f] Figure 4c.

of the reaction. The stationary structures calculated at the B3LYP/6-311++G(d,p) level are shown in Figure 5 and are representative of the corresponding structures calculated at other levels. With this basis, the calculated barriers (Table 3) differ widely; they are 34.7 (HF), 21.0 (MP2) and 5.1 kcal mol^{-1} (B3LYP), and are reduced considerably to 31.0 (HF), 34.9 (MP2), and 36.7 kcal mol^{-1} (B3LYP) compared with those found in the absence of H_2O. The reaction energies (Table 3) are essentially unchanged at the HF and MP2 levels; they are, respectively, −22.7 and −11.0 kcal mol^{-1}, (−24.8 and −9.8 kcal mol^{-1} uncatalyzed). The B3LYP product structure is somewhat more stabilized relative to reactants (20.6 kcal mol^{-1}) compared with the uncatalyzed reaction (13.8 kcal mol^{-1}). We note that the inclusion of thermodynamic corrections increases somewhat the barriers at both HF and MP2 levels, whereas the barrier decreases at the DFT level (Table 3).

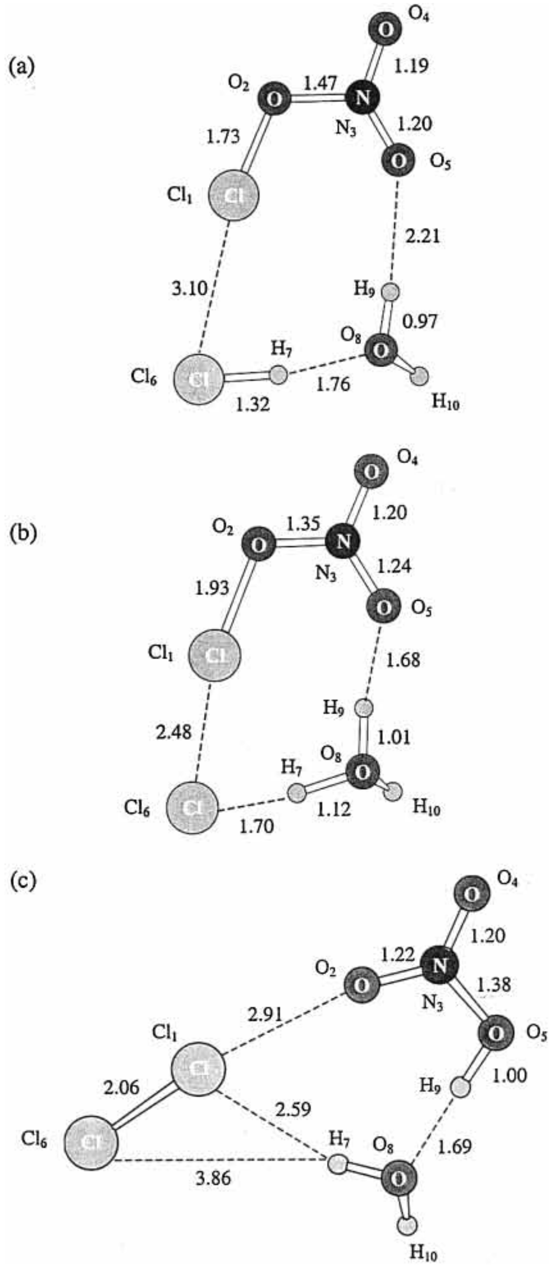

Figure 5. Stationary structures for reaction of $ClONO_2$ with HCl solvated by *one* water molecule: (a) reactants, (b) transition state, and (c) products ($Cl_2/HONO_2$).

At the DFT level, the reactant complex contains molecular $ClONO_2$, HCl, and H_2O forming a single ring structure (Figure 5a). The reaction proceeds via a proton transfer mechanism to an almost planar transition structure (Figure 5b) containing partially ionized $ClONO_2$ and essentially fully dissociated HCl. Collapse of the transition state leads to the solvated molecular product complex $Cl_2/HONO_2{\cdot}H_2O$ (Figure 5c). The structures of both $ClONO_2$ and HCl in the reactant complex (Figure 5a) are perturbed only a little from those of the isolated molecules (Table 1). The transition state (Figure 5b) highlights important differences between the catalyzed and uncatalyzed reactions. There is significant charge separation in the transition structure, with a large negative charge of -0.29 associated with the ionizing $ClONO_2$ (-0.05 reactant complex). There is also a large positive charge (0.54) on the protonated water entity ($H_2O + H_7$), in contrast to the uncatalyzed reaction where the positive charge (0.25) is on the protonated $ClONO_2$ entity. The imaginary frequency of the transition state (179i cm^{-1}, Table 3) corresponds to transfer of H_7 to the adjacent water molecule (O_8) and of Cl_1 to Cl_6, forming Cl_2. In the transition structure the length of the breaking and forming $Cl_1{-}O_2$ and $O_2{-}N_3$ bonds of $ClONO_2$ and $HONO_2$ (1.93 and 1.35 Å) are close to the MP2 values with the smaller basis (1.95 and 1.34 Å, Table 5). The transfer of the acidic proton (H_7) to the adjacent water molecule (O_8) is well advanced, with a $Cl_6{-}H_7$ distance of 1.70 Å, indicating incipient Cl^- formation. The product structure (Figure 5c), which involves the molecular acid and Cl_2, is characterized by a strong hydrogen bond between $HONO_2$ and H_2O (1.69 Å). However, Cl_2 is only weakly bound, with nonbonded $Cl_1{-}O_2$ and $Cl_1{-}H_7$ distances of 2.91 and 2.59 Å, respectively. A similar product structure is obtained at the MP2 level (Table 5).

In view of our finding that the catalysis of the $ClONO_2 +$ HCl reaction by one water molecule results in a decrease in the barrier height from 41.8 to 5.1 kcal mol^{-1} [B3LYP/6-311++G(d,p)], we now consider the catalytic effect of solvation by two water molecules.

E. $ClONO_2 + HCl{\cdot}(H_2O)_2$. Because the DFT model yields structures for the uncatalyzed and water-assisted reactions of $ClONO_2$ and HCl, close to the MP2 structures, we obtained stationary structures for the $ClONO_2 + HCl{\cdot}(H_2O)_2$ reaction at the B3LYP/6-311++G(d,p) level. However, in view of the wide variation in energetics calculated using different models, MP2 single-point energy calculations were carried out on all DFT structures with the larger 6-311++G(3df,3pd) basis [shown to more accurately describe $ClONO_2$ (Table 1)]. The free energies at the MP2 level include the thermodynamic correction from the appropriate B3LYP calculation at 180 K. We examined two possible structures in which $ClONO_2$ is solvated with two water molecules. The first, isomer 1 (Figure 6a) contains $ClONO_2$ and HCl solvated in a single ring structure, where the arrangement of the water molecules is related to a fragment excised from the surface of an ideal ice crystal (similar to that used by Bianco and Hynes[43,49] to study the hydrolysis of $ClONO_2$). Isomer 2 (Figure 7a) contains essentially the reactant structure from the reaction catalyzed by one water molecule (Figure 5a) with an additional water hydrogen bonded to O_8.

Isomer 1. The inclusion of an extra water into the ring structure (Figure 6a) results in a lowering of the barrier to 1.1 kcal mol^{-1} (B3LYP), with a facile reaction also being predicted at the MP2 level. The reaction energy (-17.5 kcal mol^{-1}, B3LYP) is a little less than for the one-water reaction (Table 3). The reactant structure (Figure 6a) can be considered as a fragment excised from the ideal ice surface[49−52] where molecular HCl is adsorbed and there is insufficient solvation to stabilize the (potential) ionized acid (H^+Cl^-). Both $ClONO_2$ and HCl are somewhat dissociated within this cluster (Table 1). Partial ionization of $ClONO_2$, induced by charge transfer, is supported by a formal charge of -0.10 associated with this species (Table 2). This result is consistent with an ab initio study of the chlorine nitrate anion by Seeley et al.,[47] where the addition of an electron to neutral $ClONO_2$ resulted in lengthening and shortening of the $Cl_1{-}O_2$ and $O_2{-}N_3$ bonds, respectively. The central feature of the predicted transition state (Figure 6b, imaginary frequency 194i cm^{-1}) is that it corresponds to a simple proton transfer from HCl to an adjacent water to generate the strong nucleophile Cl^-. The extent of ionization of $ClONO_2$ in the transition state is less than that in the one-water-assisted reaction, which is evident from the $Cl_1{-}O_2$ and $O_2{-}N_3$ bond breaking and forming distances of 1.84 and 1.39 Å, respectively. Furthermore, a formal charge of -0.18 associated with $ClONO_2$ indicates increased

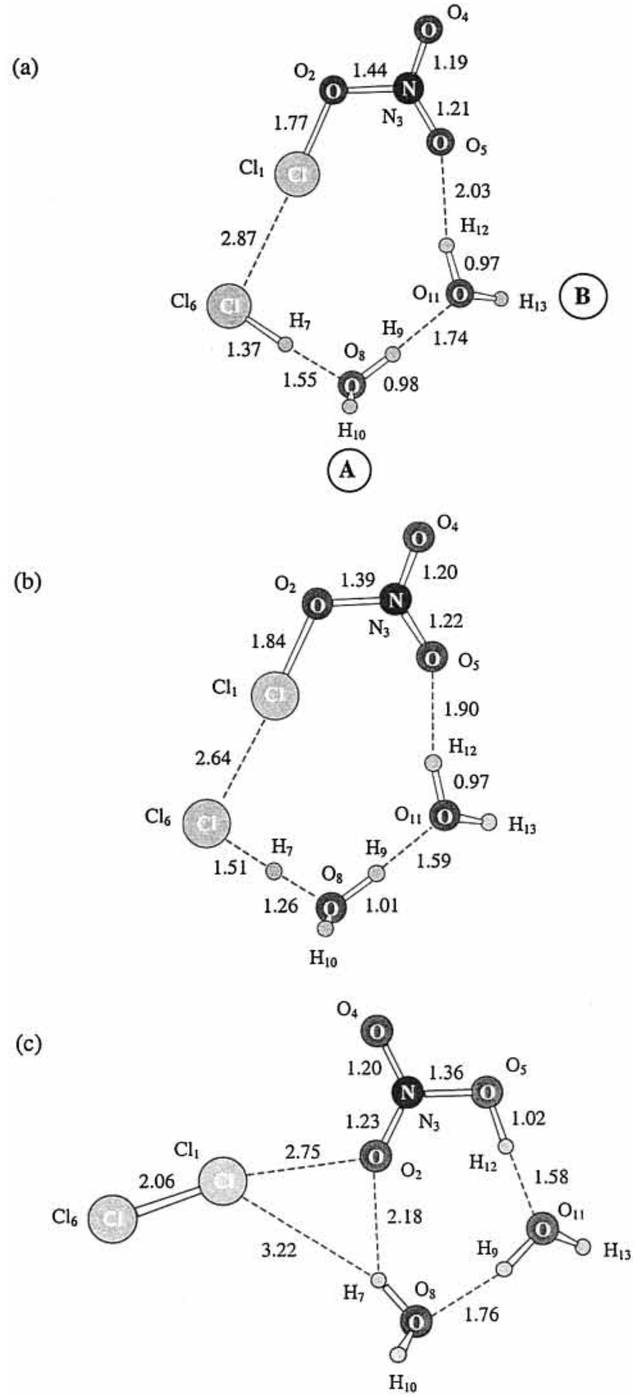

Figure 6. Stationary structures for reaction of $ClONO_2$ with HCl solvated by *two* water molecules (isomer 1): (a) reactants, (b) transition state, and (c) products ($Cl_2/HONO_2$).

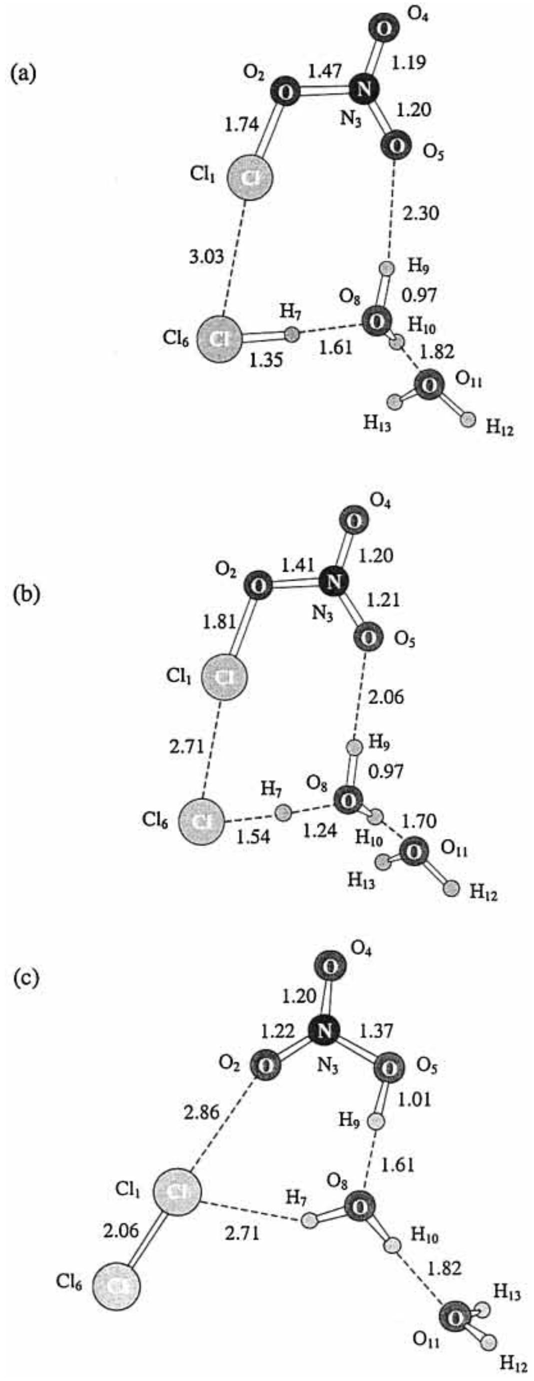

Figure 7. Stationary structures for reaction of $ClONO_2$ with HCl solvated by *two* water molecules (isomer 2): (a) reactants, (b) transition state, and (c) products ($Cl_2/HONO_2$).

charge transfer to $ClONO_2$ in the transition state compared with the reactant structure. Compared with the one-water reaction, the formation of a species akin to H_3O^+ is less well defined, with the transferring proton (H_7) being still some distance from the accepting water molecule (1.26 Å), although formal charges of 0.23 and 0.25 are associated with H_2O and H_7, respectively. A shortening of the ring hydrogen bonds is also noted [decreasing from 2.03 and 1.74 Å (reactant complex) to 1.90 and 1.59 Å (transition state), respectively]. The products of the reaction (Figure 6c) are again molecular nitric acid and Cl_2, where $HONO_2$ is solvated by two water molecules forming a hydrogen-bonded ring structure. In agreement with the one-water-assisted reaction, Cl_2 is only weakly bound to the $HONO_2\cdot(H_2O)_2$ complex, with nonbonded distances of 2.75 and 3.22 Å, respectively.

Isomer 2. The second isomer (Figure 7a) is related to the reactant structure in the one-water-catalyzed reaction (Figure 5a). We added an extra water molecule that is not directly involved in the solvating ring to examine the catalytic effect of a second solvation shell. At 180 K, isomer 2 is a little higher in energy than isomer 1 (1.3 kcal mol^{-1}). The calculated barriers are a little larger than for the reaction involving isomer 1 [i.e., 2.1 (B3LYP) and 4.8 kcal mol^{-1} (MP2)]. We now consider the stationary structures. A number of differences between the isomer 2 (Figure 7a) and isomer 1 (Figure 6a) reactant structures are evident. First, both $ClONO_2$ and HCl are ionized to a lesser extent in the isomer 2 reactant structure than in isomer 1 and

TABLE 5: Geometric Parameters for $ClONO_2$ + $HCl\cdot(H_2O)$ Reaction

	geometric parameter[a]									
method/basis set	Cl_1-O_2	O_2-N_3	N_3-O_4	N_3-O_5	O_5-H_9	O_8-H_9	O_8-H_{10}	H_7-O_8	Cl_6-H_7[b]	Cl_1-Cl_6
HF/6-311++G(d,p)										
reactants	1.667	1.362	1.162	1.173	2.283	0.944	0.941	1.977	1.282	3.596
transition state	1.885	1.285	1.165	1.222	1.618	0.991	0.950	1.002	1.948	2.361
products	3.150	1.189	1.168	1.318	0.963	1.782	0.942	0.944	4.192 (2.998)	2.002
MP2/6-31++G(d,p)										
reactants[c]	1.712	1.508	1.210	1.212	2.196	0.966	0.965	1.849	1.289	3.264
transition state	1.949	1.336	1.228	1.265	1.527	1.031	0.971	1.044	1.832	2.364
products[c]	2.898	1.236	1.221	1.382	0.998	1.701	0.965	0.968	3.685 (2.515)	2.024
B3LYP/6-311++G(d,p)										
reactants[d]	1.734	1.470	1.190	1.200	2.210	0.967	0.963	1.762	1.321	3.096
transition state[e]	1.928	1.354	1.201	1.240	1.678	1.005	0.968	1.115	1.697	2.478
products[c,f]	2.914	1.221	1.199	1.380	0.998	1.687	0.963	0.967	3.855 (2.589)	2.057

[a] Distances (Å). All structures essentially planar. Refer to Figure 5 for atom labeling. [b] (In parentheses) Cl_1-H_7 distance. [c] Nonplanar. [d] Figure 5a. [e] Figure 5b. [f] Figure 5c.

also the Cl_1-Cl_6 intermolecular distance in isomer 2 (3.03 Å) is notably longer than that in isomer 1 (2.87 Å). These differences possibly explain the small difference in barrier heights (Table 3). We located a transition state for the two-water-assisted reaction involving isomer 2 (Figure 7b). In line with the reaction for isomer 1, the transition structure essentially corresponds to a simple proton transfer. The internal hydrogen bonds have notably shortened to 1.70 and 2.06 Å (from 1.82 and 2.30, respectively, in the reactant complex), and a formal charge of −0.17 associated with $ClONO_2$ indicates charge transfer to this molecule. Collapse of the transition state yields Cl_2 and molecular $HONO_2$ in a product structure (Figure 7c) similar to that for the reaction of isomer 1 (Figure 6c) but 2.1 kcal mol^{-1} higher in energy.

We thus conclude that waters in a second solvation shell have an appreciable catalytic effect, although to a lesser extent than those directly involved in the solvating ring. We have shown that a facile reaction can occur in a relatively small model cluster, indicating the gas phase, water-catalyzed reaction of $ClONO_2$ + HCl may be important in contributing to the atmospheric activation of chlorine. However, in the reactions considered thus far, the products of the gas phase reaction involve molecular nitric acid ($HONO_2$), whereas at stratospherically relevant conditions the products of the ice-catalyzed reaction involve the ionized acid ($H_3O^+NO_3^-$).[6,13−22] Therefore, we now consider the reaction catalyzed by three and four water molecules.

F. $ClONO_2$ + $HCl\cdot(H_2O)_3$ and $ClONO_2$ + $HCl\cdot(H_2O)_4$. To investigate the reasons for the formation of the ionic products ($Cl_2/H_3O^+NO_3^-$) observed at stratospherically relevant temperatures,[6,13−22] we considered essentially two different models. The first model contains a single ring of water molecules and reactants and is related to a fragment excised from the ideal ice surface[49−52] (Figures 8 and 9). The interaction of $ClONO_2$ with complete rings containing both three or four water molecules and ionized HCl (Figures 10 and 11) was also studied. This second model has features evident on the ice surface studied by Buch et al.,[81] who report rings of water molecules large enough to accommodate several adsorbate species that are proposed as the sites for acid ionization.

Single Ring Models. Our study begins by considering a range of three- and four-water clusters analogous to those used by other authors in the study of $ClONO_2$ hydrolysis.[49−52] With the two-water reactant cluster (Figure 6a), we examined the effect of solvation by a single water molecule at A or B, at distances typical of hydrogen bonds in hexagonal ice (∼1.65 Å). Optimization of the initial structures solvated at A or B led directly to molecular product clusters ($Cl_2/HONO_2$) analogous to those found in the one- and two-water-catalyzed reactions, with no stable reactant structure. However the addition of a third ring-water molecule (cluster 1, Figure 8) leads to a stable reactant structure containing essentially $ClONO_2$ and HCl, where the arrangement of the water molecules is related to a fragment excised from the ideal ice surface with HCl adsorbed atop on oxygen. In view of the very low barrier found for the two-water-assisted reaction (Table 3), a facile reaction is probable for this cluster and no transition state search was carried out.

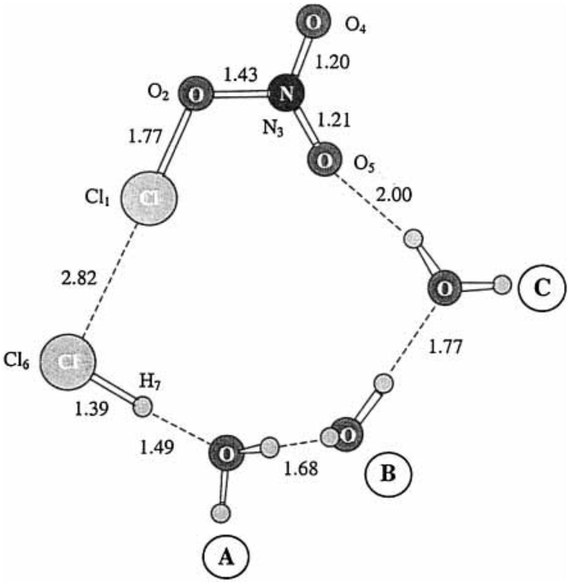

Figure 8. $ClONO_2$ and HCl solvated by *three* water molecules (cluster 1).

We examined the further solvation of our three-water reactant structure (cluster 1, Figure 8) with extra-ring water molecules placed at A, B, and C. As expected, solvation at C, remote from the site of acid ionization, yields an analogous structure containing un-ionized HCl. However, solvation at A or B, close to the proton acceptor of the ionizing acid (HCl), leads to structures containing ionized HCl, as indicated in cluster 2 (Figure 9a) containing a well-defined hydroxonium ion and strongly polarized $ClONO_2$. Within this reactant structure, a strong interaction between the transferring Cl_1 and both the forming nitrate and attacking Cl^- is evident from Cl_1-O_2 and Cl_1-Cl_6 bond breaking and forming distances of 2.01 and 2.38 Å, respectively. A shortened O_2-N_3 bond of 1.33 Å (1.52 Å free molecule) indicates incipient nitrate formation, and further

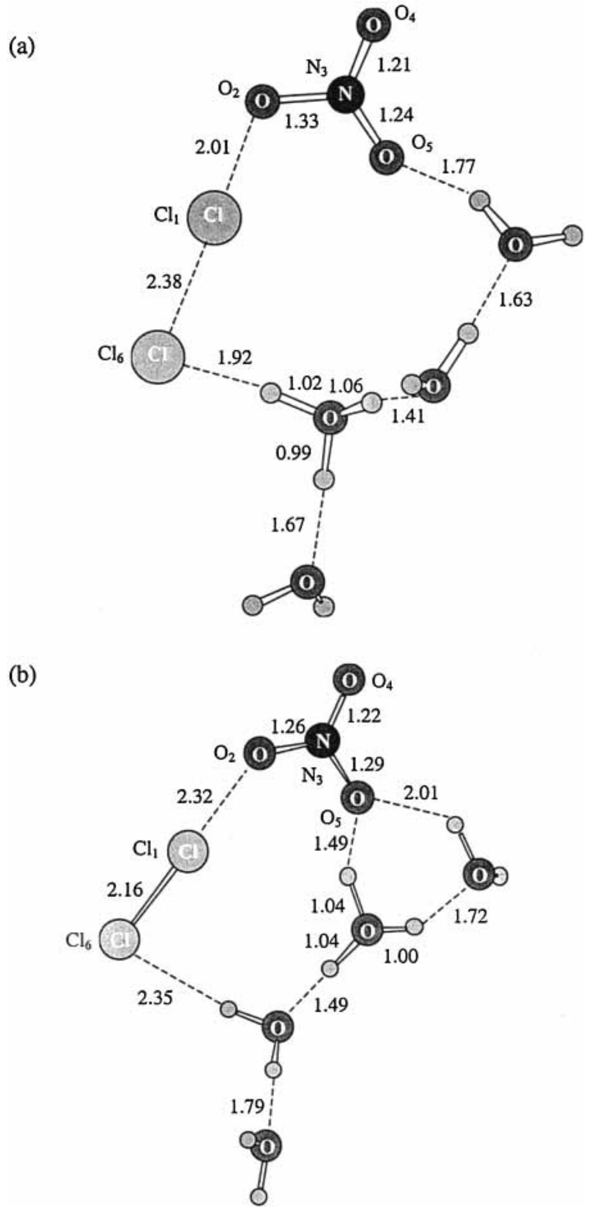

Figure 9. $ClONO_2$ and *ionized* HCl solvated by *four* water molecules: (a) reactant structure (cluster 2) and (b) product structure (cluster 3).

evidence of the formation of hydroxonium ion is afforded by a charge of 0.61 associated with the H_3O entity (Table 6). The calculated charges (Table 6) support the idea of charge transfer from the chloride to $ClONO_2$ being -0.30 on Cl_6 and -0.40 on $ClONO_2$. However, a Cl_1-Cl_6 distance 0.33 Å greater than in free Cl_2 indicates the reaction is far from complete. In view of the very low barrier predicted for similar structures involving two water molecules (Table 3), no transition state search was carried out because a low barrier is also probable for this system. Given that the arrangement of the water molecules in the reactant-like structure is able to support the ionized acid, $(H_3O^+Cl^-)$ and strongly ionized $ClONO_2$, we investigated the possibility that a product-like structure containing the ionized nitric acid $(H_3O^+NO_3^-)$ may also be stable within a related structure.

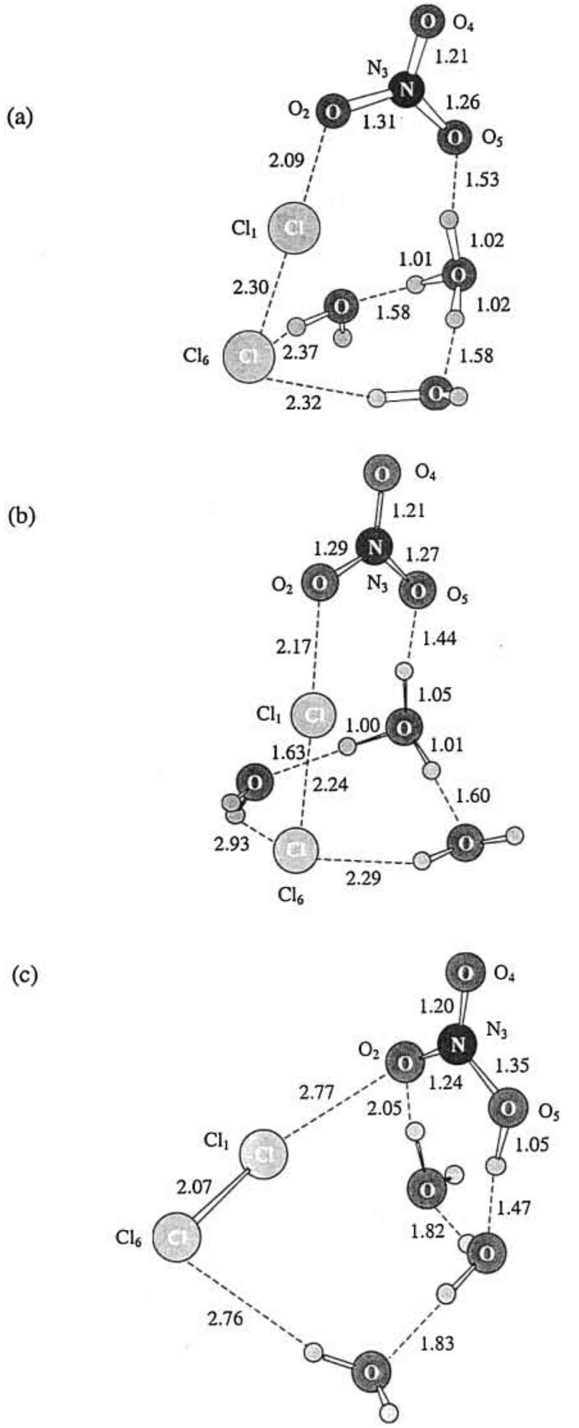

Figure 10. Stationary structures for reaction of $ClONO_2$ with *ionized* HCl solvated by *three* water molecules: (a) reactants (cluster 4), (b) transition state, and (c) products ($Cl_2/HONO_2$).

We identified a product-like structure containing the ionized nitric acid contact ion pair (cluster 3, Figure 9b). This new ion-pair structure was obtained from the first ion-pair structure by a manual shift of a proton of the hydroxonium ion onto an adjacent water molecule. As far as overall energetics are concerned, the product-like structure (Figure 9b) is 5.5 kcal mol^{-1} (9.1 kcal mol^{-1}, MP2) more stable than the reactant-like cluster 2 (Figure 9a). Within this structure, formal charges of 0.71 (H_3O) and -0.57 (NO_3) indicate well-defined nitrate and hydroxonium ions that are separated by a relatively short hydrogen bond of length 1.49 Å. A nonbonded Cl_1-O_2 distance of 2.32 Å results in a notable distortion of the Cl_1-Cl_6 distance (2.16 Å) from the free molecule case (2.05 Å). These findings suggest that four water molecules are required to support the ionization of HCl and the formation of the ionized product nitric acid $(H_3O^+NO_3^-)$ which is in agreement with previous calculations.[66,67] However, to understand the reaction on the PSC

TABLE 6: Mulliken Charges (e) B3LYP/6-311++G(d,p) of Reactant Pair (Figure 2) in Clusters

	atomic charge[a]							total fragment charge					
cluster	Cl_1	O_2	N_3	O_4	O_5	Cl_6	H_7	$ClONO_2$	HCl	Cl_2	H_3O	NO_3	$HONO_2$
					single ring models								
					$ClONO_2 + HCl\cdot(H_2O)_3$								
1[b]	0.11	0.11	−0.38	0.04	0.02	−0.27	0.24	−0.10	−0.03				
					$ClONO_2 + HCl\cdot(H_2O)_4$								
2[c] reactants	0.00	0.08	−0.37	−0.02	−0.09	−0.30		−0.40		−0.30	0.61	−0.40	
3[d] products	−0.04	−0.01	−0.27	−0.06	−0.23	−0.13				−0.17	0.71	−0.57	
					ice surface ring models								
					$ClONO_2 + HCl\cdot(H_2O)_3$								
4[e] reactants	−0.04	0.08	−0.33	−0.02	−0.17	−0.29		−0.48		−0.33	0.78	−0.44	
transition state	−0.06	0.04	−0.32	−0.02	−0.17	−0.21		−0.53		−0.27	0.76	−0.47	
products	−0.06	−0.08	−0.31	0.02	−0.07	0.02				−0.04			0.01
					$ClONO_2 + HCl\cdot(H_2O)_4$								
5[f]	−0.02	0.08	−0.38	−0.01	−0.10	−0.37		−0.43		−0.39	0.77	−0.41	
6[g]	−0.03	0.05	−0.32	−0.01	−0.14	−0.31		−0.45		−0.34	0.76	−0.42	
					$ClONO_2 + HCl\cdot(H_2O)_5$								
7[h]	−0.03	−0.01	−0.29	−0.04	−0.26	−0.14				−0.17	0.65	−0.60	

[a] Refer to Figures for atom labeling. [b] Figure 8. [c] Figure 9a. [d] Figure 9b. [e] Figure 10. [f] Figure 11a. [g] Figure 11b. [h] Figure 12b.

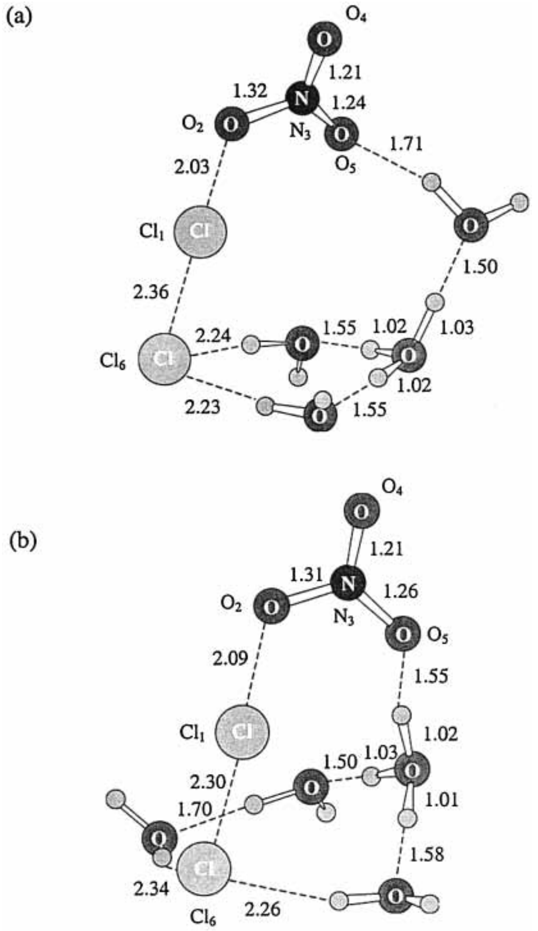

Figure 11. $ClONO_2$ and *ionized* HCl solvated by *four* water molecules: (a) reactant structure (cluster 5) and (b) reactant structure (cluster 6).

surface, we must increase the size of the first solvation shell of Cl^-, which may be important in determining the barrier to reaction.

Ice Surface Ring Models. We now consider a second type of cluster related to the rings identified on the 140 K annealed ice surface studied by Buch et al.[81] In a recent study of the direct reaction, Bianco and Hynes[43] identified two possible scenarios regarding the fate of the ionized acid HCl. The first involves ionization to produce the contact ion pair, $H_3O^+Cl^-$, or alternatively there is a high probability that proton transfer will occur yielding a solvent-separated ion pair. In both cases, desolvation of Cl^- is required for reaction. Thus, we investigated both the structural and energetic effects of increasing the first solvation shell around Cl^- from one to two waters and of separating the ion pair ($H_3O^+Cl^-$) by up to two layers of water molecules.

Our first model system contains $ClONO_2$ solvated by three water molecules (cluster 4, Figure 10a). Within this structure, $ClONO_2$ is coordinated to the ionized acid, where the ion pair ($H_3O^+Cl^-$) is separated by a single layer of water molecules, and the nucleophile Cl_6 is solvated by two waters. Energetically, this structure is 5.0 kcal mol^{-1} (2.1 kcal mol^{-1}, MP2) higher in energy than in the three-water structure (cluster 1, Figure 8) containing un-ionized HCl; the small difference in stability is probably due to the strained hydrogen bonds in cluster 4. Compared with the three-water structure (Figure 8) containing un-ionized HCl, cluster 4 (Figure 10a) contains a significantly more polarized $ClONO_2$ molecule, with respectively lengthened and shortened Cl_1-O_2 and O_2-N_3 bonds (2.09 and 1.31 Å) and a forming Cl_1-Cl_6 bond (2.30 Å) that is a little more product-like. Charge transfer from the attacking nucleophile (Cl_6) is well advanced with a formal charge (Table 7) of −0.48 associated with the $ClONO_2$ entity. In line with this, the large positive charge of 0.78 on H_3O indicates a well-defined hydroxonium ion. Calculation of the transition state (Figure 10b) leading to the molecular products ($Cl_2/HONO_2$) yields an essentially zero barrier at both the B3LYP and MP2 levels (Table 3). The charge distribution within this transition structure is essentially the same as that in the reactant structure [−0.47 (NO_3) and 0.76 (H_3O)], and the transferring Cl_1 is approximately midway between O_2 of the departing nitrate and Cl_6 of the forming Cl_2. The product structure (Figure 10c) is formed by the transfer of a proton from the hydroxonium ion adjacent to O_5 of the nitrate to yield solvated $HONO_2$ and Cl_2, and is 17.4 kcal mol^{-1} lower in energy than the reactant cluster (24.4 kcal mol^{-1}, MP2). We note that in the transition structure identified, the developing nitrate is poorly solvated, whereas on the PSC surface, the presence of additional solvating waters around the reactive site may stabilize the developing nitrate entity and collapse to ionized nitric acid ($H_3O^+NO_3^-$).

To investigate the structural effects of increasing the number

TABLE 7: Internal and Free Energies (Hartrees) of Clusters

	internal energy (0 K)		free energy (180 K)	
cluster	B3LYP/6-311++G(d,p)	MP2/6-311++G(3df,3pd)[a]	B3LYP/6-311++G(d,p)	MP2/6-311++G(3df,3pd)[b]
single ring models				
$ClONO_2 + HCl·(H_2O)_3$				
1[c]	−1430.785544	−1428.842877	−1430.712002	−1428.769335
$ClONO_2 + HCl·(H_2O)_4$				
2[d] reactants	−1507.266260	−1505.180172	−1507.165753	−1505.079665
3[e] products	−1507.275071	−1505.194843	−1507.174447	−1505.094219
ice surface ring models				
$ClONO_2 + HCl·(H_2O)_3$				
4[f] reactants	−1430.801110	−1428.853780	−1430.720034	−1428.772704
transition state	−1430.800428	−1428.853727	−1430.719856	−1428.773155
products	−1430.813415	−1428.877286	−1430.747735	−1428.811606
$ClONO_2 + HCl·(H_2O)_4$				
5[g]	−1507.277148	−1505.193708	−1507.172641	−1505.089201
6[h]	−1507.280516	−1505.197735	−1507.176147	−1505.093366
$ClONO_2 + HCl.(H_2O)_5$				
7[i]	−1583.757755	−1581.541919	−1583.629823	−1581.413987

[a] Single-point energy evaluation using B3LYP/6-311++G(d,p) structure. [b] Includes thermodynamic correction at B3LYP/6-311++G(d,p) level. [c] Figure 8. [d] Figure 9a. [e] Figure 9b. [f] Figure 10. [g] Figure 11a. [h] Figure 11b. [i] Figure 12b.

of solvation shells around the reacting species, we located two more minimum energy structures containing four water molecules. The first, cluster 5 (Figure 11a), is related to the three-water cluster (Figure 10a) but with a single water inserted between the hydroxonium ion and the developing nitrate of the ionizing $ClONO_2$. The extra water essentially represents a surface-bound water above the plane of the ring solvating the ionized acid. Cluster 6 (Figure 11b) is also related to the three-water cluster (Figure 10a), but with an extra water molecule inserted into the ring solvating the acid such that the ion pair ($H_3O^+Cl^-$) is now separated by single and double layers of water molecules. Both these clusters have features evident on the ice surface studied by Buch et al.[81]

As far as overall energetics are concerned (Table 7) an extra internal hydrogen bond results in clusters 5 and 6 being, respectively, 4.3 and 6.5 kcal mol^{-1} lower in energy than the single-ring cluster 2 (Figure 9a). Turning now to consider the structures of these species, in cluster 6 (Figure 11b) for example, $ClONO_2$ is significantly ionized. A breaking Cl_1-O_2 bond of length 2.09 Å and a net charge of −0.45 (Table 6) associated with the $ClONO_2$ entity support the concept of charge transfer from Cl_6 affecting ionization of $ClONO_2$. A shortened O_2-N_3 bond of 1.31 Å indicates incipient nitrate formation, and a charge of 0.76 on H_3O is evidence for a well-defined hydroxonium ion. Having considered the $ClONO_2$ + HCl reaction catalyzed by both three and four water molecules in two different types of structure related to the PSC surface, we now examine the reaction in water clusters with structural arrangements of water molecules closely related to that of hexagonal ice.[52]

G. $ClONO_2 + HCl·(H_2O)_5$. We investigated the reactivity of $ClONO_2$ and $H_3O^+Cl^-$ in a five-water cluster where the arrangement of the water molecules is structurally related to ordinary hexagonal ice. Figure 1 depicts a proton-ordered phase of hexagonal ice with the model cluster water positions shown. Surface bilayer water molecules (A, B) were removed to accommodate $ClONO_2$. In view of the findings of Buch et al.,[81] our model system could be present either as part of a ring structure reported on the annealed nanocrystal surface or as a surface defect found on the unannealed surface.

The initial reactant structure was constructed by taking our structure containing $ClONO_2$ hydrated by six water molecules (Figure 12a), used previously in the study of the hydrolysis reaction,[52,53] and replacing the nucleophilic water molecule by Cl^- and protonating the adjacent water molecule to form the contact ion pair $H_3O^+Cl^-$. Optimization of this structure led directly to the product-like structure (cluster 7, Figure 12b) containing Cl_2 and ionized nitric acid ($H_3O^+NO_3^-$). A strong interaction between Cl_2 and both the nitrate and hydroxonium

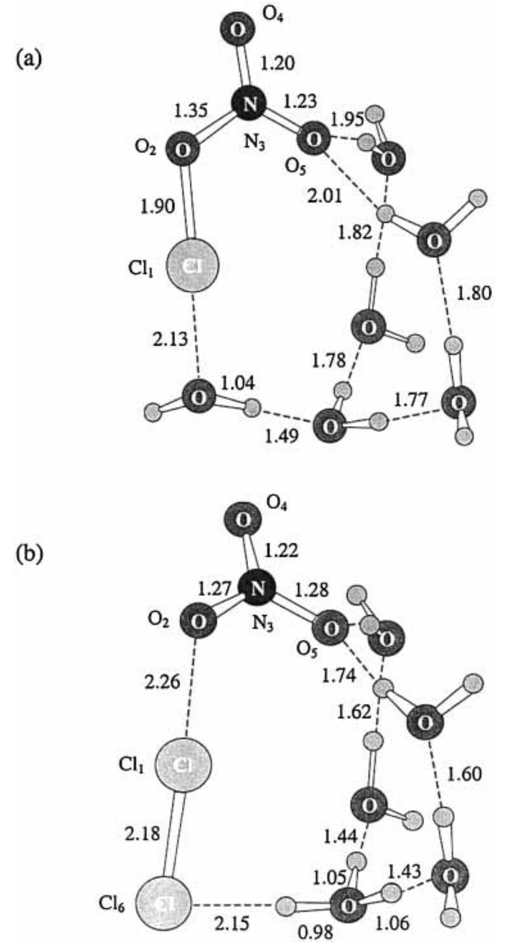

Figure 12. (a) Initial hydrolysis structure, $ClONO_2$ solvated by *six* water molecules; (b) $ClONO_2$ and *ionized* HCl solvated by *five* water molecules, product structure (cluster 7, $Cl_2/H_3O^+NO_3^-$).

ions is evident from the extended Cl_1-Cl_6 bond length of 2.18 Å [free molecule, 2.05 Å, B3LYP/6-311++G(d,p)]. Further evidence of the strong interaction with the ionized acid is afforded by a charge of −0.17 on Cl_2. Thus, $ClONO_2$ reacts spontaneously with HCl to form ionic products in a five-water cluster structurally related to hexagonal ice. However, the initial reactant-like structure contains Cl^- solvated by only a single water, whereas the first solvation shell of Cl^- may contain up to three waters on a PSC surface.[39−41,43] In view of these results, we investigated the reactivity of $ClONO_2$ in a corresponding seven-water cluster in which two additional waters were added to complete the first solvation shell of Cl^-, at distances typical of H−Cl nonbonded distance found in the clusters discussed so far (~2.35 Å). Optimization of this cluster at the B3LYP/6-311++G(d,p) level leads to some distortion of the initial arrangement of water molecules, however, the calculations indicate that the final product structure contains species akin to ionized nitric acid ($H_3O^+NO_3^-$) and Cl_2, which is very close to those identified in the five-water cluster (Figure 12b). These findings suggest the reaction on the PSC surface will proceed essentially spontaneously, even when Cl^- has a complete first solvation shell.

5. Discussion

We begin by commenting on the choice of basis set and model of electron correlation. For $ClONO_2$ itself (Table 1), we find that the DFT (B3LYP) method with the 6-311++G(d,p) basis yields a structure of essentially the same quality as the CCSD(T)/TZ2P method[45] and is in good agreement with the experimental vibrationally averaged gas-phase structure.[45] As far as the uncatalyzed (Table 4, Figure 4) and the one-water-assisted (Table 5, Figure 5) reactions of $ClONO_2$ with HCl are concerned, the transition structures calculated at the DFT level are very close to the corresponding MP2 structures. In agreement with recent studies,[52,53,65] the 6-311++G(d,p) basis was used to more accurately model the potential energy surface, because both polarization and diffuse functions are required to describe hydrogen bonded systems, with smaller basis sets tending to predict preferential stabilization of zwitterionic structures. Finally, we note that the HF, MP2, and DFT models yield somewhat different barriers (Table 3).

The calculations herein reveal a number of important features concerning the reaction of $ClONO_2$ with HCl in small water clusters. Importantly, we observed a change from a molecular mechanism for the gas-phase reaction to an ionic mechanism for the PSC-catalyzed reaction.

For the smaller systems studied, containing one to three solvating waters, the reactions involve $ClONO_2$ and un-ionized HCl. These model reactions indicate that the gas-phase or homogeneous reaction of $ClONO_2$ with HCl may also be important in increasing active chlorine reservoirs. The calculated barriers [Table 3, B3LYP/6-311++G(d,p)] show that the involvement of catalytic waters reduces the barrier from 41.8 (uncatalyzed) to 1.1 kcal mol^{-1} on the inclusion of only two water molecules, and further increasing the size of the water cluster to three water molecules leads to an essentially spontaneous reaction. These findings are consistent with an ab initio study by Xu and Zhao[55] in which a facile reaction is also predicted. Although at present there are no available experimental data concerning the rate of the reaction for comparison, the prompt appearance of Cl_2 (180 K) reported by Horn et al.[17] suggests a ready reaction. The proposed increase in the electrophilicity of the Cl atom of $ClONO_2$[16,17,52] resulting from ionization along the Cl_1-O_2 bond is evident from our reactant structures (Figures 5a, 6a, and 7a), and supporting this is a small transfer of charge from the substrate (HCl water cluster) to $ClONO_2$. This effect, although small, is evidence for a change toward an ionic mechanism as the number of solvating waters is increased. A central feature of the transition states is that they are somewhat akin to simple proton transfers from HCl to $ClONO_2$ in the absence of water (Figure 4b) and to an adjacent water molecule in the water-assisted reactions (Figure 5b, 6b, and 7b).

The PSC-catalyzed reaction, differs from the gas-phase reaction in that the reactant structures now contain $H_3O^+Cl^-$ and strongly ionized $ClONO_2$ (Figures 9a, 10a, 11a, and 11b). We considered two different types of model system. The first model involves single rings of water molecules and is related to fragments excised from an ideal ice surface, as used in previous studies of the hydrolysis reaction.[49−52] The second model is related to the rings identified on the 140 K annealed ice surface studied by Buch et al.[81] These minimum-energy structures have revealed at a molecular level a number of important details concerning the mechanism of the reaction and are in agreement with previous theoretical findings.[43]

(i) Laboratory studies and MD simulations[36−41] suggest that at stratospheric conditions ionized HCl is present at the ice surface. In agreement with this result, our reactant structures (Figures 9a, 10a, 11a, and 11b), which are representative of the local adsorption sites on a PSC surface, all contain $H_3O^+Cl^-$. The reactant clusters also account for the ionized acid forming a contact-ion pair (Figure 9a) or the solvent-separated ion pair (Figures 10a, 11a, and 11b). Comparison of the four-water clusters 2 and 6 suggests that the separation of $H_3O^+Cl^-$ by up to two waters leads to a stronger nucleophile and thus to increased charge transfer, resulting in increased ionization along the $Cl-ONO_2$ bond. Bianco and Hynes[43] suggest the separation of the ion pair would lead to the reaction proceeding as reaction 3. Thus, we conclude that the solvent separation of the $H_3O^+Cl^-$ pair is an important step for a facile reaction on a PSC surface.

(ii) As far as the reaction on the PSC surface is concerned, desolvation of Cl^- may be an essential step for the reaction. Bianco and Hynes studied the $ClONO_2$ + HCl reaction involving nine water molecules at the MP2/(SBK+*,6-31G+G*)//HF(HW*,3-21G) level,[43] where the nucleophile Cl^- has a first solvation shell. In our study, we attempted to quantify the effect on reactivity of increasing the size of the Cl^- solvation shell from one (Figure 9a) to three (seven-water cluster, related to Figure 12b) water molecules. For the four-water cluster (Figure 9a), the first solvation shell of Cl^- contains a single water and a low barrier is predicted for the reaction to the product-like structure (Figure 9b). Increasing the first solvation shell to two waters, as in clusters 4, 5, and 6 (Figures 10a, 11a, and 11b), does not radically alter the reactivity because an essentially zero barrier is calculated for the three-water-catalyzed reaction (Figure 10, Table 3). For the reaction catalyzed by five water molecules (Figure 12b) leading to the ionic products with zero barrier, increasing the solvation shell of Cl^- from one to three waters has little effect. These findings suggest that complete solvation of Cl^-, may not be as important as the separation of the ion pair $H_3O^+Cl^-$.

(iii) Experimental findings indicate that for the heterogeneously catalyzed $ClONO_2$ + HCl reaction, the final reaction product involve the ionized acid $H_3O^+NO_3^-$.[6,13−22] We identified two such clusters, one involving four waters where the ionized nitric acid forms a contact ion pair (Figure 9b) and the other, in which the ion pair is effectively separated by two solvation shells (Figure 12b). For a three-water cluster (Figure 10a), which initially contains $H_3O^+Cl^-$, the product structure involves Cl_2/$HONO_2$ (Figure 10c). Analysis of the transition structure (Figure 10b) for this reaction reveals insufficient solvation of the forming nitrate, and thus additional surface-bound waters may be required to participate in the stabilization of the developing nitrate on the PSC surface.

(iv) Finally we comment on the energetics of the PSC-catalyzed reaction. An ab initio investigation by Bianco and Hynes[43] involving a nine-water cluster yielded a barrier of 6.4 kcal mol^{-1}. In agreement with this, our calculations indicate the reaction on the PSC surface may actually proceed spontaneously, particularly if the reaction involves the solvent-separated ion pair ($H_3O^+Cl^-$) and proceeds as reaction 3.

In summary, our calculations have shown that the homogeneous or gas-phase reaction between $ClONO_2$ and un-ionized HCl, when catalyzed by only two waters, can occur readily at stratospherically relevant temperatures. This reaction may be an important contributor to the increase in active chlorine in the stratosphere. In larger clusters related to PSC ice aerosols, the reaction between $ClONO_2$ and the ionized acid ($H_3O^+Cl^-$) can proceed essentially spontaneously, whereby solvent separation of acid, leads to the reaction proceeding as in eq 3. Here the formation of an ionic product requires the participation of more water molecules than are needed to promote the reaction. However, our central finding of atmospheric importance is that the reaction of $ClONO_2$ with HCl, a key element in the proposed formation of the ozone hole, proceeds essentially spontaneously via an ionic pathway in water clusters of a relatively small critical size.

Acknowledgment. We thank EPSRC for support of this research and Dr. J. C. Whitehead for helpful discussion.

References and Notes

(1) Molina, M. J.; Rowland, F. S. *Nature* **1974**, *249*, 810.

(2) Tolbert, M. A. *Science* **1994**, *264*, 527.

(3) Solomon, S.; Garcia, R. R.; Rowland, F. S.; Wuebbles, D. J. *Nature* **1986**, *321*, 755.

(4) Solomon, S. *Rev. Geophys.* **1988**, *26*, 131.

(5) Solomon, S. *Nature* **1990**, *347*, 347.

(6) Molina, M. J.; Tso, T.-L.; Molina, L. T.; Wang, F. C.-Y. *Science* **1987**, *238*, 1253.

(7) Cicerone, R. J. *Science* **1987**, *237*, 35.

(8) Turco, R. P.; Toon, O. B.; Hamill, P. J. *Geophys. Res.* **1989**, *94*, 16 493.

(9) McElroy, M. B.; Salawitch, R. J.; Wofsy, S. C. *Geophys. Res. Lett.* **1986**, *13*, 1296.

(10) Henderson, G. S.; Evans, W. F. J.; McConnell, J. C. *J. Geophys. Res.* **1990**, *95*, 1899.

(11) Wennberg, P. O.; Cohen, R. C.; Stimpfle, R. M.; Koplow, J. P.; Anderson, J. G.; Salawitch, R. J.; Fahey, D. W.; Woodbridge, E. L.; Keim, E. R.; Gao, R. S.; Webster, C. R.; May, R. D.; Toohey, D. W.; Avallone, L. M.; Proffitt, M. H.; Loewenstein, M.; Podolske, J. R.; Chan, K. R.; Wofsy, S. C. *Science* **1994**, *266*, 398.

(12) Crutzen, P. J.; Arnold, F. *Nature* **1986**, *324*, 651.

(13) Banham, S. F.; Horn, A. B.; Koch, T. G.; Sodeau, J. R. *Faraday Discuss.* **1995**, *100*, 321.

(14) Sodeau, J. R.; Horn, A. B.; Banham, S. F.; Koch, T. G. *J. Phys. Chem.* **1995**, *99*, 6258.

(15) Koch, T. G.; Banham, S. F.; Sodeau, J. R.; Horn, A. B.; McCoustra, M. R. S.; Chesters, M. A. *J. Geophys. Res.* **1997**, *102*, 1513.

(16) Horn, A. B.; Sodeau, J. R.; Roddis, T. B.; Williams, N. A. *J. Chem. Soc., Faraday Trans.* **1998**, *94*, 1721.

(17) Horn, A. B.; Sodeau, J. R.; Roddis, T. B.; Williams, N. A. *J. Phys. Chem. A* **1998**, *102*, 6107.

(18) Hanson, D. R.; Ravishankara, A. R. *J. Geophys. Res.* **1991**, *96*, 5081.

(19) Leu, M.-T. *Geophys. Res. Lett.* **1988**, *15*, 17.

(20) Chu, L. T.; Leu, M.-T.; Keyser, L. F. *J. Phys. Chem.* **1993**, *97*, 12 798.

(21) Tolbert, M. A.; Rossi, M. J.; Malhotra, R.; Golden, D. M. *Science* **1987**, *238*, 1258.

(22) Hanson, D. R.; Ravishankara, A. R. *J. Phys. Chem.* **1992**, *96*, 2682.

(23) Hanson, D. R.; Ravishankara, A. R. *J. Phys. Chem.* **1994**, *98*, 5728.

(24) Hanson, D. R. *J. Phys. Chem. A* **1998**, *102*, 4794.

(25) Zhang, R.; Jayne, J. T.; Molina, M. J. *J. Phys. Chem.* **1994**, *98*, 867.

(26) Zhang, R.; Leu, M.-T.; Keyser, L. *J. Phys. Chem.* **1994**, *98*, 13 563.

(27) Oppliger, R.; Allanic, A.; Rossi, M. J. *J. Phys. Chem. A* **1997**, *101*, 1903.

(28) Barone, S. B.; Zondlo, M. A.; Tolbert, M. A. *J. Phys. Chem. A* **1997**, *101*, 8643.

(29) Zondlo, M. A.; Barone, S. B.; Tolbert, M. A. *J. Phys. Chem. A* **1998**, *102*, 5735.

(30) Wincel, H.; Mereand, E.; Castleman, Jr., A. W. *J. Phys. Chem. A* **1997**, *101*, 8248.

(31) Nelson, C. M.; Okumura, M. *J. Phys. Chem.* **1992**, *96*, 6112.

(32) Van Doren, J. M.; Viggiano, A. A.; Morris, R. A. *J. Am. Chem. Soc.* **1994**, *116*, 6957.

(33) Schindler, T.; Berg, C.; Niedner-Schatteburg, G.; Bondybey, V. E. *J. Chem. Phys.* **1996**, *104*, 3998.

(34) La. Manna, G. *J. Mol. Struct. (THEOCHEM)* **1994**, *309*, 31.

(35) Wofsy, S. C.; Molina, M. J.; Salawitch, R. J.; Fox, L. E.; McElroy, M. B. *J. Geophys. Res.* **1988**, *93*, 2442.

(36) Gertner, B. J.; Hynes, J. T. *Faraday Discuss.* **1998**, *110*, 301.

(37) Rieley, H.; Aslin, H. D. *J. Chem. Soc., Faraday Trans.* **1995**, *91*, 2349.

(38) Horn, A. B.; Chesters, M. A.; McCoustra, M. R. S., Sodeau, J. R. *J. Chem. Soc.*, *Faraday Trans.* **1992**, *88*, 1077.

(39) Delzeit, L.; Powell, K.; Uras, N.; Devlin, J. P. *J. Phys. Chem. B* **1997**, *101*, 2327.

(40) Graham, J. D.; Roberts, J. T. *J. Phys. Chem.* **1994**, *98*, 5974.

(41) Delzeit, L.; Rowland, B.; Devlin, J. P. *J. Phys. Chem.* **1993**, *97*, 10 312.

(42) George, S. M.; Livingston, F. E. *Surf. Rev. Lett.* **1994**, *4*, 771.

(43) Bianco, R.; Hynes, J. T. *J. Phys. Chem. A* **1999**, *103*, 3797.

(44) Haas, B.-M.; Crellin, K. C.; Kuwata, K. T.; Okumura, M. *J. Phys. Chem.* **1994**, *98*, 6740.

(45) Lee, T. J. *J. Phys. Chem.* **1995**, *99*, 1943.

(46) Ying, L. M.; Zhao, X. S. *J. Phys. Chem A* **1997**, *101*, 6807.

(47) Seeley, J. V.; Miller, T. M.; Viggiano, A. A. *J. Chem. Phys.* **1996**, *105*, 2127.

(48) Lee, T. J.; Rice, J. E. *J. Phys. Chem.* **1993**, *97*, 6637.

(49) Bianco, R.; Hynes, J. T. *J. Phys. Chem. A* **1998**, *102*, 309.

(50) Xu, S. C.; Zhao, X. S. *J. Phys. Chem. A* **1999**, *103*, 2100.

(51) Xu, S. C.; Zhao, X. S. *Acta Phys.-Chim. Sinica* **1998**, *14*, 988.

(52) McNamara, J. P.; Hillier, I. H. *J. Phys. Chem. A* **1999**, *103*, 7310.

(53) McNamara, J. P.; Tresadern, G.; Hillier, I. H. *Chem. Phys. Lett.* **1999**, *310*, 265.

(54) Mebel, A. M.; Morokuma, K. *J. Phys. Chem. A* **1996**, *100*, 2985.

(55) Xu, S. C.; Zhao, X. S. *Acta Phys.-Chim. Sinica* **1998**, *14*, 5.

(56) Akhmatskaya, E. V.; Apps, C. J.; Hillier, I. H.; Masters, A. J.; Palmer, I. J.; Watt, N. E.; Vincent, M. A.; Whitehead, J. C. *J. Chem. Soc., Faraday Trans.* **1997**, *93*, 2775.

(57) Beichert, P.; Schrems, O. *J. Phys. Chem. A* **1998**, *102*, 10 540.

(58) Geiger, F. M.; Hicks, J. M.; de Dios, A. C. *J. Phys. Chem. A* **1998**, *102*, 1514.

(59) Packer, M. J.; Clary, D. C. *J. Phys. Chem.* **1995**, *99*, 14 323.

(60) Robinson Brown, A.; Doren, D. J. *J. Phys. Chem. B* **1997**, *101*, 6308.

(61) Koput, J.; Peterson, K. A. *Chem. Phys. Lett.* **1998**, *283*, 139.

(62) Hanway, D.; Tao, F.-M. *Chem. Phys. Lett.* **1998**, *285*, 459.

(63) Estrin, D. A.; Kohanoff, J.; Laria, D. H.; Weht, R. O. *Chem. Phys. Lett.* **1997**, *280*, 280.

(64) Vincent, M. A.; Palmer, I. J.; Hillier, I. H.; Akhmatskaya, E. V. *J. Am. Chem. Soc.* **1998**, *120*, 3431.

(65) Smith, A.; Vincent, M. A.; Hillier, I. H. *J. Phys. Chem. A* **1999**, *103*, 1132.

(66) Planas, M.; Lee, C.; Novoa, J. J. *J. Phys. Chem.* **1996**, *100*, 16495.

(67) Lee, C.; Sosa, C.; Planas, M.; Novoa, J. J. *J. Chem. Phys.* **1996**, *104*, 7081

(68) Robertson, S. H.; Clary, D. C. *Faraday Discuss.* **1995**, *100*, 309.

(69) Ying, L. M.; Zhao, X. S. *J. Phys. Chem. A* **1997,** *101*, 3569.

(70) Ando, K.; Hynes, J. T. *J. Phys. Chem. B* **1997**, *101*, 10 464.

(71) Xu, S. C.; Zhao, X. S. *Acta Phys.-Chim. Sinica* **1999**, *15*, 193.

(72) Xu, S. C. *J. Chem. Phys.* **1999**, *111*, 2242.

(73) Lee, C.; Vanderbilt, D.; Laasonen, K.; Car, R.; Parrinello, M. *Phys. Rev. B* **1993**, *47*, 4863.

(74) Bernal, J. D.; Fowler, R. H. *J. Chem. Phys.* **1933**, *8*, 515.

(75) Davidson, E. R.; Morokuma, K. *J. Chem. Phys.* **1984**, *81*, 3741.

(76) Materer, N.; Starke, U.; Barbieri, A.; Van Hove, M. A.; Somorjai, G. A.; Kroes, G.-J.; Minot, C. *J. Phys. Chem.* **1995**, *99*, 6267.

(77) Silva, S. C.; Devlin, J. P. *J. Phys. Chem.* **1994**, *98*, 10 847.

(78) Devlin, J. P.; Buch, V. *J. Phys. Chem.* **1995**, *99*, 16 534.

(79) Devlin, J. P.; Buch, V. *J. Phys. Chem. B* **1997**, *101*, 6095.

(80) Rowland, B.; Kadagathur, N. S.; Devlin, J. P.; Buch, V.; Feldman, T.; Wojcik, M. J. *J. Phys. Chem.* **1995**, *99*, 8328.

(81) Buch, V.; Delzeit, L.; Blackledge, C.; Devlin, J. P. *J. Phys. Chem.* **1996**, *100*, 3732.

(82) Casassa, S.; Ugliengo, P.; Pisani, C. *J. Chem. Phys.* **1997**, *106*, 8030.

(83) Morrison, I.; Li, J.-C.; Jenkins, S.; Xantheas, S. S.; Payne, M. C. *J. Phys. Chem. B* **1997**, *101*, 6146.

(84) Moore Plummer, P. L. *J. Phys. Chem. B* **1997**, *101*, 6247.

(85) Moore Plummer, P. L. *J. Phys. Chem. B* **1997**, *101*, 6251.

(86) Frisch, M. J.; Trucks, G. W.; Schlegel, H. B.; Gill, P. M. W.; Johnson, B. G.; Robb, M. A.; Cheeseman, J. R.; Keith, T. A.; Petersson, G. A.; Montgomery, J. A.; Raghavachari, K.; Al-Laham, M. A.; Zakrzewski, V. G.; Ortiz, J. V Foresman, J. B.; Cioslowski, J.; Stefanov, B. B.; Nanayakkara, A.; Challacombe, M.; Peng, C. Y.; Ayala, P. Y.; Chen, W.; Wong, M. W.; Andres, J. L.; Replogle, E. S.; Gomperts, R.; Martin, R. L.; Fox, D. J.; Binkley, J. S.; Defrees, D. J.; Baker, J.; Stewart, J. P.; Head-Gordon, M.; Gonzalez G.; Pople, J. A. *Gaussian94*, revision E.1; Gaussian, Inc.; Pittsburgh, PA, 1995.

(87) Frisch, M. J.; Trucks, G. W.; Schlegel, H. B.; Scuseria, G. E.; Robb, M. A.; Cheeseman, J. R.; Zakrzewski, V. G.; Montgomery, J. A.; Stratmann, R. E.; Burant, J. C.; Dapprich, S.; Millam, J. M.; Daniels, A. D.; Kudin, K. N.; Strain, M. C.; Farkas, O.; Tomasi, J.; Barone, V.; Cossi, M.; Cammi, R.; Mennucci, K.; Pomelli, C.; Adamo, C.; Clifford, S.; Ochterski, J.; Petersson, G. A.; Ayala, P. Y.; Cui, Q.; Morokuma, K.; Malick, D. K.; Rabuck, A. D.; Raghavachari, K.; Foresman, J. B.; Cioslowski, J.; Ortiz, J. V.; Sefanov, B. B.; Liu, G.; Liashenko, A.; Piskorz, P.; Komaromi, I.; Gomperts, R.; Martin, R. L.; Fox, D. J.; Keith, T.; Al-Laham, M. A.; Peng, C. Y.; Nanayakkara, A.; Gonzalez, C.; Challacombe, M.; Gill, P. M. W.; Johnson, B. G.; Chen, W.; Wong, M. W.; Andres, J. L.; Head-Gordon, M.; Replogle E. S.; Pople, J. A. *Gaussian98*, revision A.1; Gaussian, Inc.; Pittsburgh, PA, 1998.

(88) Lee, C.; Yang. W.; Parr, R. G. *Phys. Rev. B* **1988**, *37*, 785

(89) Miehlich, B.; Savin, A.; Stoll, H.; Preuss, H. *Chem. Phys. Lett.* **1989**, *157*, 200.

(90) Becke, A. D. *J. Chem. Phys.* **1993**, *98*, 5648.

(91) Møller, C.; Plesset, M. S. *Phys. Rev.* **1934**, *46*, 618.